*J. Synchrotron Rad.* (1998). **5**, 1090–1092

# Development of scanning X-ray microscopes for materials science spectromicroscopy at the Advanced Light Source

**T. Warwick,[a*] H. Ade,[b] S. Cerasari,[a,c] J. Denlinger,[d] K. Franck,[a] A. Garcia,[a,b] S. Hayakawa,[e] A. Hitchcock,[f] J. Kikuma,[g] S. Klingler,[a] J. Kortright,[a] G. Morisson,[a] M. Moronne,[a] E. Rightor,[h] E. Rotenberg,[a] S. Seal,[a] H.-J. Shin,[a,i] W. F. Steele[a] and B. P. Tonner[j]**

*[a]Lawrence Berkeley National Laboratory, University of California, Berkeley, California, USA, [b]Department of Physics, North Carolina State University, Raleigh, North Carolina, USA, [c]Universita di Trieste, Trieste, Italy, [d]University of Michigan, Ann Arbor, Michigan, USA, [e]School of Engineering, University of Tokyo, Tokyo, Japan, [f]Department of Chemistry, McMaster University, Hamilton, Ontario, Canada, [g]ASAHI Chemical Industry Company, Fuji shi, Japan, [h]DOW Chemical, Freeport, Texas, USA, [i]Pohang Accelerator Laboratory, POSTECH, Pohang, Korea, and [j]Department of Physics, University of Wisconsin, Milwaukee, Wisconsin, USA. E-mail: warwick@lbl.gov*

(*Received 4 August 1997; accepted 21 October 1997*)

The development of two zone-plate microscopes for X-ray spectroscopic analysis of materials is described. This pair of instruments will provide imaging NEXAFS analysis of samples in transmission at atmospheric pressure and imaging XPS and NEXAFS analysis of sample surfaces in a UHV environment.

**Keywords: spectromicroscopy; NEXAFS; XPS; zone plates.**

## 1. Introduction

Third-generation synchrotron sources of soft X-rays provide an excellent opportunity to apply established X-ray spectroscopic materials analysis techniques to surface imaging on a sub-micron scale. This paper describes development at the Advanced Light Source (ALS) using Fresnel zone-plate lenses with soft X-rays (Kirz, 1973) to produce a sub-micron spot of photons for use in scanning microscopy. Several groups have developed microscopes using this technique (Kirz *et al.*, 1995; Ko *et al.*, 1995; Marsi *et al.*, 1997). A specimen is rastered in the focused X-ray spot and a detector signal is acquired as a function of position to generate an image. Spectroscopic capability is added by holding the small spot on a feature of interest and scanning through the spectrum.

We are pursuing two spectroscopic techniques to provide a capability for light-element analysis in materials science.

(i) Near-edge X-ray absorption spectroscopy (NEXAFS) (Stohr, 1992) gives characteristic information about light-element chemistry and the interaction of these atoms with their neighbors. Organic molecules typically exhibit identifiable peaks corresponding to molecular orbitals localized at specific atomic sites. Their spectra can be calculated (Carravetta *et al.*, 1995; Urquhart *et al.*, 1995), and exhibit strong dependence on the polarization of the photon and the orientation of the molecules. Ionically bonded species have absorption spectra that show strong charge-state dependence. Crystal field effects are seen in ordered solids (deGroot, 1994).

(ii) X-ray photoelectron spectroscopy (XPS) gives quantitative measurements of the concentration of species and quantitative measurements of core-level chemical shifts. Surface imaging XPS can be performed with commercial equipment at a spatial resolution of about 10 μm. In this work we extend the technique to explore sub-micron spatial scales.

These two spectroscopies are applied in a pair of scanning zone-plate microscopes which operate in tandem at undulator beamline 7.0 (Warwick *et al.*, 1995) at the ALS. Fig. 1 shows this facility. The count rates in these microscopes are about ten times higher than previously available.

## 2. Scanning transmission X-ray microscope (STXM)

Fig. 2 illustrates the zone-plate scheme employed in the STXM. The lens is outside a 160 nm-thick $Si_3N_4$ vacuum window. We are presently using lenses with 80 nm outer zone width, and a corresponding diffraction limit to the spatial resolution of about 100 nm. Images made of fractured thin windows (100 nm $Si_3N_4$) show blurring consistent with an X-ray spot size of 150 nm FWHM. The order-sorting aperture (OSA) is precisely posi-

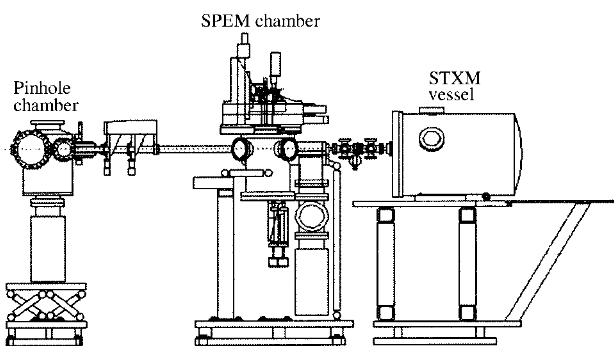


**Figure 1**
The tandem layout of the two microscopes. The upstream microscope is a UHV scanning photoelectron microscope (SPEM). The photon beam passes through the SPEM chamber to the STXM, which is the last item in the beamline.

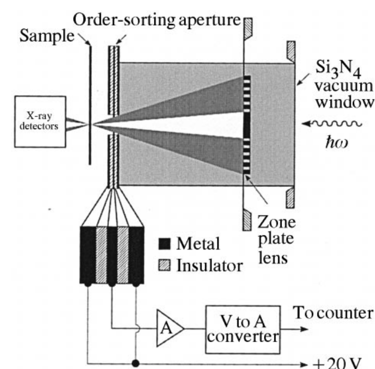


**Figure 2**
Schematic arrangement of the windows, lens, order-sorting aperture (OSA), sample and detector in the STXM.

© 1998 International Union of Crystallography
Printed in Great Britain – all rights reserved

tioned on the optical axis (±2 μm) to allow only the first-order diffracted focus to reach the sample. This aperture is a photosensitive element which generates a signal (a few pA) proportional to the illumination intensity for spectral normalization against the effects of low-frequency (<10 Hz) beam motion in the beamline, which cannot be averaged over the counting interval (a few hundred milliseconds). We have measured $2 \times 10^7$ photons $s^{-1}$ with a spectral width 1/3000 in the zone-plate first-order focus spot at 300 eV, with the storage ring running at 1.5 GeV, 400 mA. At higher photon energies the intensity increases, as the windows become more transparent, until the beamline output decreases above 500 eV (Warwick *et al.*, 1995). Images are typically acquired with a counting time of 10 ms per pixel. NEXAFS spectra are acquired with a counting time of several hundred milliseconds per energy point. Coordinated undulator and monochromator moves take about 250 ms to complete, during which time a fast mechanical shutter closes to protect radiation-sensitive samples from unnecessary exposure.

The transmission geometry is the most efficient use of photons for an absorption spectrum, well suited to radiation-sensitive organic samples.

Measurements in transmission are bulk sensitive, so that surface contamination is not a concern; this allows the operation of the microscope at atmospheric pressure, in air or helium, with hydrated samples for problems in environmental science.

The most difficult mechanism involved in this microscope is the flexure which translates the zone plate longitudinally through 0.5 mm to remain in focus as the photon energy is changed during a NEXAFS scan. This mechanism inevitably has some unwanted sideways run-out (about 0.4 μm) which is reproducible and compensated by programmed sideways motion of the sample during the spectral scan. The resulting lock-in (0.2 μm) allows spectra to be measured with some confidence on features uniform over regions as small as 0.5 μm. We are presently making a transition to finer zone plates (spatial resolution improved by a factor of two) with shorter focal lengths (by a factor of four) so that the spatial resolution will be improved and this difficult translation will be smaller.

Photons are detected in transmission by one of two detectors.

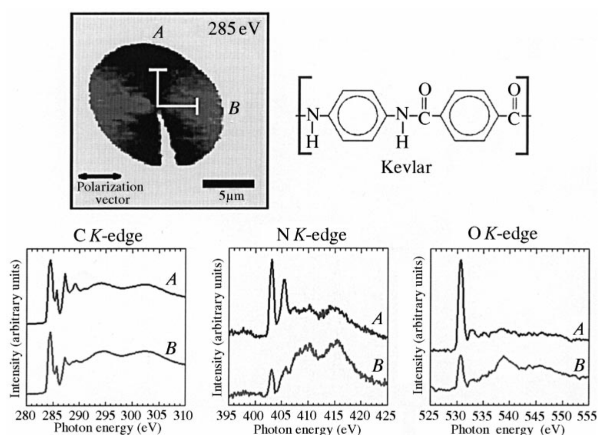


**Figure 3**
A sectioned Kevlar fiber measured with the STXM. Absorption spectra are measured at points *A* and *B*, showing the dependence on the angle between the photon polarization vector (horizontal) and the radially oriented polymer chains. Spectra are shown for each of the main atomic species present. The polarization contrast reverses between the $\pi$ and $\sigma$ orbital peaks.

(i) An analog silicon photodiode (from International Radiation Detectors, Torrance, CA 90505, USA) for full intensity measurements. This detector is essentially 100% efficient above 100 eV except for a thin oxide layer. It is typically used with a 10 ms amplifier time constant.

(ii) A photomultiplier tube collecting visible light from a phosphor (P43) behind the sample. This scheme is under development but shows an overall X-ray counting efficiency of 25% and is linear beyond 1 MHz counting rate.

Fig. 3 shows a case study illustrating the STXM capabilities. Kevlar fibers have been studied before (Ade & Hsiao, 1993). In this case the polarization/orientation sensitivity is explored at the *K*-edge of three atoms in the molecule: C, O and N. The latter two measurements require a pure helium environment to remove atmospheric absorption effects.

### 3. Scanning photoemission microscope (SPEM)

Fig. 4 illustrates the zone-plate scheme employed in SPEM. Here the sample is stationary during imaging and the zone plate is rastered in the illumination field to carry the focused spot across the sample surface. The illumination is of the order of 1 mm diameter and the raster range is 80 × 80 μm. The electron spectrometer can view the entire range of the image area and collects photoelectrons at 60° from the sample normal. The OSA is within 0.5 mm of the sample surface, and the zone-plate assembly is cut back on one side to allow a line of sight for the spectrometer. NEXAFS capability is included by means of a flexure to carry the zone plate 0.5 mm longitudinally to retain the focus condition as the photon energy changes. The OSA moves away from its optimum longitudinal position during a NEXAFS scan but not so far as to intercept the first-order light.

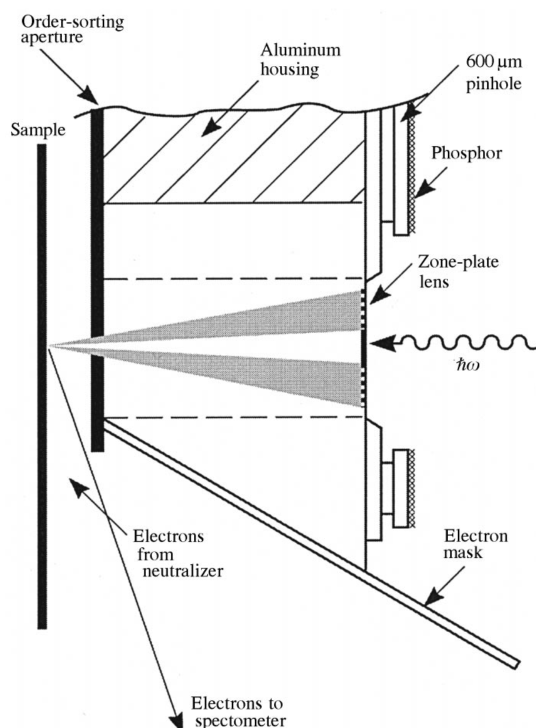


**Figure 4**
Schematic arrangement of the lens, order-sorting aperture (OSA), sample and spectrometer in the SPEM.

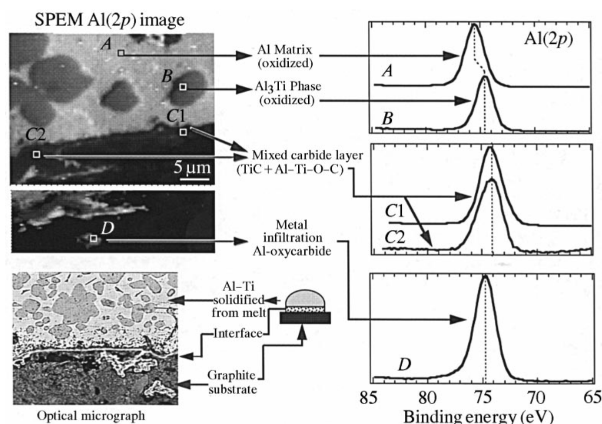


**Figure 5**
SPEM images and Al $2p$ XPS spectra from a metallurgical study of Al/Ti melt interactions with solid graphite. Early results provide quantitative chemical shifts and stoichiometry of alloy precipitates and carbide formation at the interface.

The OSA is fixed to the zone plate, with the focal length built into the assembly. Different photon energies require different zone-plate/OSA combinations with different built-in focal lengths (*e.g.* 620 eV for survey spectra including O 1*s* photoelectrons, 270–310 eV for C *K*-edge NEXAFS measurements). Five zone plates will be mounted together on a monolithic array with precisely parallel optical axes (to $\pm 1$ mrad), interchangeable under computer control. So far we have operated the microscope with three zone plates/OSAs aligned in this way. SPEM allows us to perform quantitative XPS measurements of atomic concentration and core-level chemical shifts over regions of the sample surface as small as the spatial resolution of the zone-plate lens (currently X-ray spots smaller than 0.3 μm have been achieved). The zone-plate array can be lowered out of the beam and the sample surface can be observed with the same video system, allowing visible fiducial marks on the sample to be used to position the region of interest within the $100 \times 100$ μm range of the scan stage. XPS spectra are measured with typical photo-peak count rates of 70000 counts $s^{-1}$ (Au 4*f* at 420 eV photon energy).

Sample charging is partially neutralized by the proximity of the zone-plate assembly to the sample surface (which serves as a source of low-energy electrons) and by an electron flood gun. Remaining charging shifts are corrected relative to the photo-emission peaks of contaminant carbon or to a Fermi edge. Sample sputtering and annealing is provided in a preparation chamber adjacent to the microscope chamber. The instrument operates at $5 \times 10^{-10}$ torr.

Fig. 5 shows a SPEM case study in which an Al/Ti melt has been allowed to solidify on a graphite substrate (Sobczak *et al.*, 1995). The image of the polished section shows the aluminium metal, precipitates of $Al_3Ti$ alloy and the graphite interface, with carbide formation. Different core-level chemical shifts are observed from the Al, the $Al_3Ti$ alloy and the carbide region. Topography is visible in the image because of the sideways collection of electrons. The harder alloy precipitates are proud of the metal surface after polishing. In this case sputtering has removed the adventitious carbon contamination but the surface is still oxidized.

## References

Ade, H. & Hsiao, B. (1993). *Science*, **262**, 1427–1429.
Carravetta, V., Agren, H., Petterson, L. & Vahtras, O. (1995). *J. Chem. Phys.* **102**, 5589–5594.
deGroot, F. (1994). *J. Electron. Spectrosc. Relat. Phenom.* **76**, 529–535.
Kirz, J. (1973). *J. Opt. Soc. Am.* **64**, 301–309.
Kirz, J., Jacobsen, C. & Howells, M. (1995). *Q. Rev. Biophys.* **28**, 33–130.
Ko, C., Kirz, J., Ade, H., Johnson, E., Hulbert, S. & Andersen, E. (1995). *Rev. Sci. Instrum.* **66**, 1416–1418.
Marsi, M., Casalis, L., Gregoratti, L., Gunther, S., Kolmakov, A., Kovac, J., Lonza, D. & Kiskinova, M. (1997). *J. Electron Spectrosc. Relat. Phenom.* **84**, 73–83.
Sobczak, N., Gorny, Z., Rohatgi, P., Koigzeh, M. & Radzimill, W. (1995). *Proc. Cast Composties '95*, Zakopane, Poland.
Stohr, J. (1992). *NEXAFS Spectroscopy*, *Springer Series in Surface Sciences* 25. Heidelberg: Springer.
Urquhart, S., Hitchcock, A., Rightor, E. & Priester, R. (1995). *Polym. Sci.* B**33**, 1603–1609.
Warwick, T., Heimann, P., Mossessian, D., McKinney, W. & Padmore, H. (1995). *Rev. Sci. Instrum.* **66**, 2037–2040.